



---

VanNieuwenhove I, Salomon A, Peters K, Graulus G, Martins JC, Frankel D, Kersemans K, DeVos F, VanVlierberghe S, Dubruel P. [Gelatin- and starch-based hydrogels. Part A: Hydrogel development, characterization and coating](#). *Carbohydrate Polymers* 2016

DOI: <http://dx.doi.org/10.1016/j.carbpol.2016.06.098>

**Copyright:**

© 2016. This manuscript version is made available under the [CC-BY-NC-ND 4.0 license](#)

**Date deposited:**

05/07/2016

**Embargo release date:**

27 June 2017



This work is licensed under a [Creative Commons Attribution-NonCommercial-NoDerivatives 4.0 International licence](#)

**Gelatin- and starch-based hydrogels. Part A: Hydrogel development, characterization and coating.**

Ine Van Nieuwenhove<sup>1</sup>, Achim Salamon<sup>2</sup>, Kirsten Peters<sup>2</sup>, Geert-Jan Graulus<sup>1</sup>,  
José C. Martins<sup>3</sup>, Daniel Frankel<sup>4</sup>, Ken Kersemans<sup>5</sup>, Filip De Vos<sup>5</sup>, Sandra Van Vlierberghe<sup>1,6\*</sup>,  
Peter Dubruel<sup>1\*</sup>

\* Corresponding authors: [sandra.vanvlierberghe@ugent.be](mailto:sandra.vanvlierberghe@ugent.be) , [peter.dubruel@ugent.be](mailto:peter.dubruel@ugent.be)

- 1) Polymer Chemistry & Biomaterials Group - Ghent University,  
Krijgslaan 281, Building S4-Bis, BE-9000 Ghent
- 2) Department of Cell Biology - Rostock University Medical Center,  
Schillingallee 69, D-18057 Rostock
- 3) NMR and Structure Analysis Research Group - Ghent University  
Krijgslaan 281, Building S4, BE-9000 Ghent
- 4) School of Chemical Engineering and Advanced Materials - University of Newcastle,  
Mertz Court, Claremont Road, UK-NE1 7RU Newcastle Upon Tyne
- 5) Laboratory of Radiopharmacy - Ghent University  
Ottergemsesteenweg 460, BE-9000 Ghent
- 6) Brussels Photonics Team – Vrije Universiteit Brussel  
Pleinlaan 2, BE-1050 Brussels

## Abstract

The present work aims at constructing the ideal scaffold matrix of which the physico-chemical properties can be altered according to the targeted tissue regeneration application. Ideally, this scaffold should resemble the natural extracellular matrix (ECM) as close as possible both in terms of chemical composition and mechanical properties. Therefore, hydrogel films were developed consisting of methacrylamide-modified gelatin and starch-pentenoate building blocks because the ECM can be considered as a crosslinked hydrogel network consisting of both polysaccharides and structural, signaling and cell-adhesive proteins. For the gelatin hydrogels, three different substitution degrees were evaluated including 31%, 72% and 95%. A substitution degree of 32% was applied for the starch-pentenoate building block. Pure gelatin hydrogels films as well as interpenetrating networks with gelatin and starch were developed. Subsequently, these films were characterized using gel fraction and swelling experiments, high resolution-magic angle spinning  $^1\text{H}$  NMR spectroscopy, rheology, infrared mapping and atomic force microscopy. The results indicate that both the mechanical properties and the swelling extent of the developed hydrogel films can be controlled by varying the chemical composition and the degree of substitution of the methacrylamide-modified gelatin applied. The storage moduli of the developed materials ranged between 14 and 63 kPa. Phase separation was observed for the IPNs for which separated starch domains could be distinguished located in the surrounding gelatin matrix. Furthermore, we evaluated the affinity of aggrecan for gelatin by atomic force microscopy and radiolabeling experiments. We found that aggrecan can be applied as a bioactive coating for gelatin hydrogels by a straightforward physisorption procedure. Thus, we achieved distinct fine-tuning of the physico-chemical properties of these hydrogels which render them promising candidates for tissue engineering approaches.

**Key words:** gelatin, starch, biomaterials, aggrecan, tissue engineering

Formatted: Font: (Default) Times New Roman, 12 pt

## 1. Introduction

The lack of acutely available organs for transplantation is a worldwide issue which is even expected to worsen as the world population ages. Tissue engineering is an approach aiming at bridging this gap.(Furth, Atala, & Van Dyke, 2007; Griffith & Naughton, 2002; Langer R, 1993; Langer, 1997; Lemons, 2013) In this approach, cells are seeded onto scaffolds or implants to develop into functional tissues.(Drury & Mooney, 2003; Gomillion & Burg, 2006; C. Liu, Xia, & Czernuszka, 2007; Lutolf & Hubbell, 2005; Peters et al., 2009) In addition, an increasing number of procedures can be found in literature which rely on the application of stem cells.(Barry & Murphy, 2004; Gomillion & Burg, 2006; Griffith & Naughton, 2002; Jeffrey M. Gimble et al., 2007; Peters et al., 2009) Using mesenchymal stem cells (MSC), the present study aims at a scaffold guided strategy towards tissue regeneration. The constructed scaffold is a three-dimensional matrix serving as a surrogate extracellular matrix (ECM) enabling cell attachment and promoting cell proliferation as well as differentiation. The design of a scaffold resembling the natural ECM is preferred in order to mimic as closely as possible the natural aqueous environment that cells are experiencing.(Chen, Wang, Wei, Mo, & Cui, 2010; Kim, Kim, & Salih, 2005; Kuo, Chen, Hsiao, & Chen, 2015) This natural ECM can be considered as a crosslinked hydrogel network consisting of polysaccharides as well as structural, signaling and cell-adhesive proteins. Taking this knowledge into consideration, it is of great interest to evaluate the potential of polymer networks mimicking this ECM composition. Therefore, gelatin and starch are applied as natural building blocks in the present work, representing both the protein and polysaccharide constituent of the natural ECM.

Gelatin is derived from collagen, which is the most abundant structural protein in mammals.(Di Lullo, Sweeney, Korkko, Ala-Kokko, & San Antonio, 2002) In addition, it is generally non-immunogenic and retains informational signals including an arginine-glycine-aspartic acid (RGD) sequence which promotes cell adhesion, differentiation and proliferation.(Gautam, Dinda, & Mishra, 2013) These properties and its unique gel-forming ability render gelatin an interesting biopolymer towards tissue engineering applications.(Awad, Quinn Wickham, Leddy, Gimble, & Guilak, 2004; Dubruel et al., 2007; Li et al., 2005; Nichol et al., 2010) Starch, on the other hand, consists of a mixture of the polysaccharides amylose and amylopectin. The relative ratio of amylose to amylopectin strongly depends on the starch source considered. The application of starch offers several advantages including its biodegradability and ease of processing.(Azevedo, Gama, & Reis, 2003; Puppi, Chiellini, Piras, & Chiellini, 2010) Starch-based polymers as well as blends have already been introduced as promising biomaterials for bone and cartilage tissue engineering applications due to these advantages. For instance, Mendes et al. (2001) showed the potential of starch/ethylene vinyl alcohol blends reinforced with hydroxyapatite for temporary bone replacement implants.(Mendes et al., 2001) Raafat et al. (2013) developed a hydrogel series composed of starch/N-vinylpyrrolidone which were proven to exhibit *in vitro* bioactivity and blood compatibility.(Raafat, Eldin, Salama, & Ali, 2013) Moreover, gelatin and starch are often

87 combined for several food processing applications.(Burey, Bhandari, Rutgers, Halley, & Torley,  
88 2009; Firoozmand, Murray, & Dickinson, 2009; MARRS, 1982)

89 In this work, hydrogels were developed consisting of either a gelatin phase or the combination of  
90 both a starch and a gelatin phase. In the latter case, these hydrogels are so-called interpenetrating  
91 polymer networks (IPNs) if the appropriate crosslinking strategy is applied ensuring both  
92 building blocks to be covalently crosslinked but not bonded to each other.(V et al., 2007) The  
93 potential of gelatin hydrogels in contact with adipose tissue derived mesenchymal stem cells  
94 (adMSCs) was already demonstrated by Peters et al. (2009) towards the adhesion of these  
95 cells.(Peters et al., 2009) Therefore, we selected the gelatin hydrogels as reference material for  
96 the IPNs of starch and gelatin. Pure starch hydrogels were not applied as these hydrogels were  
97 shown to be too brittle to process them in hydrogel films. To the best of our knowledge, we first  
98 reported on the combination of starch and gelatin in IPNs for the purpose of tissue engineering  
99 applications. Indeed, previous results reported by Van Nieuwenhove et al. (2015) on starch-based  
100 hydrogels were promising since the hydrogels developed in contact with adMSC were shown to  
101 be biocompatible.(Van Nieuwenhove et al., 2015)

102 IPNs have gained an increased attention the last decades mainly due to their high potential as  
103 hydrogels for biomedical applications.(Dragan, 2014) However, most of the hybrid IPNs  
104 hydrogels, reported in literature, are obtained by either combining various polysaccharides or  
105 synthetic polymers and proteins with synthetic polymers.(Dragan, 2014; La Gatta, Schiraldi,  
106 Esposito, D'Agostino, & De Rosa, 2009; Peng, Yu, Mi, & Shyu, 2006; Pescosolido et al., 2011)  
107 Only a few papers report on the combination of proteins and polysaccharides for the construction  
108 of (semi)-IPNs.(Cui, Jia, Guo, Liu, & Zhu, 2014; Y. Liu & Chan-Park, 2009; Picard, Doumèche,  
109 Panouillé, & Larreta-Garde, 2010; Turgeon & Beaulieu, 2001)

110 The present work focusses on the construction of the ideal scaffold matrix of which the physico-  
111 chemical properties can be altered according to the targeted tissue regeneration application. The  
112 latter is highly relevant as natural tissue is also characterized by different mechanical properties.  
113 Thus, altering the mechanical properties of the constructed hydrogel films is of great interest. For  
114 instance breast tissue, mainly composed of adipose tissue, is characterized by a storage modulus  
115 of 3.2 kPa(Abbas, Judit, & Donald, 2007), whereas the storage modulus of articular cartilage is in  
116 the range of 2 to 7 GPa(Silver, Bradica, & Tria, 2002). Due to their soft and rubbery consistence,  
117 hydrogels do not reveal such high storage moduli. However, these hydrogels can still be  
118 applicable as coating onto implants to target orthopedic applications.

119 For this reason, hydrogel films were prepared with varying chemical composition (i.e. ratio  
120 between gelatin and starch phase) and varying degree of substitution (DS) of the gelatin phase  
121 applied. First, gelatin and starch were chemically modified with photo-crosslinkable moieties.  
122 This modification enables their subsequent processing into hydrogel films and ensures sufficient  
123 stability of the materials upon *in vitro* application. In addition, the present work will evaluate  
124 whether a bioactive coating of aggrecan, the main articular cartilage constituent, can be deposited

onto the materials via physisorption. More specifically, liquid atomic force microscopy and radiolabeling experiments will be performed to study this hydrogel coating.

## **2. Experimental section**

### **2.1. Materials**

For all the synthesis experiments, gelatin (type B), from bovine bone origine, was applied (Rousselot, Gent, Belgium). Furthermore, dimethyl sulfoxide (DMSO, 99.85%) was purchased from Acros (Geel, Belgium) and purified via distillation before use. Irgacure® 2959 was applied as photo-initiator (BASF, Kaisten, Switzerland) and dithiothreitol (Fisher Scientific, Erembodegem, Belgium) was used as a bifunctional thiol-based crosslinker agent. All other chemicals were purchased from Sigma Aldrich (Bornem, Belgium) and were used as received unless stated otherwise. The radiolabeling experiments were performed using Iodogen (1,3,4,6-tetrachloro-3a,6a-diphenyl-glycouril) obtained from Pierce (USA) and using a radioiodide solution (125I: Perkin Elmer, Massachusetts, USA).

### **2.2. Synthesis of hydrogel building blocks**

Both the pentenoate-modified starch (SP) and the methacrylamide-modified gelatin (gel-MA) were synthesized as described earlier.(Peters et al., 2009; Van Nieuwenhove et al., 2015) In brief, corn starch was dissolved in DMSO (5 w/v%, 70 °C), a catalytic amount of dimethylaminopyridine was added and the reaction mixture was stirred for 20 minutes. Subsequently, 4-pentenoic anhydride (37.5 equivalents with respect to the saccharide units) was added and reacted overnight. The purified product was obtained via precipitation in ethanol, followed by dialysis against double distilled water (MWCO: 12,000 – 14,000 Da) and freeze-drying by means of a Christ freeze-dryer alpha 2-4-LSC.

For the gelatin derivatives, the amount of crosslinkable side chains was adjusted by varying the amount of methacrylic anhydride added. Three different modifications were performed using 0.5, 1 and 2.5 equivalents methacrylic anhydride added with respect to the primary amines present along the gelatin backbone.

### **2.3. Hydrogel production**

Hydrogel films were prepared through covalent crosslinking. For this purpose, a gel-MA solution (10 w/v%) was crosslinked via photo-induced polymerization in the presence of 2 mol% Irgacure® 2959 upon applying UV-A irradiation for 30 minutes (with an intensity of 10 mW/cm<sup>2</sup> and a wavelength range of 250-450 nm). IPNs were obtained by the addition of one equivalent of DTT and Irgacure® 2959 to various SP (5 w/v%) and gel-MA solutions (10 w/v%) which were

subsequently exposed to UV-A irradiation. The addition of DTT is needed as the crosslinking of SP occurred via a radical thiol-ene reaction.

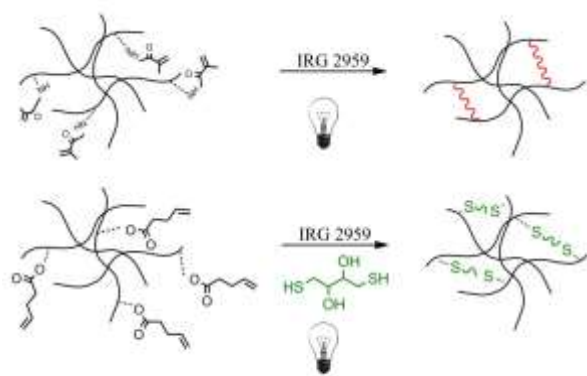


**Figure 1** UV-Crosslinking of methacrylamide-modified gelatin solution (top) upon the addition of Irgacure 2959® and starch-pentenoate (below) upon the addition of Irgacure 2959® and a bifunctional thiolcrosslinker.

## 2.4. Characterization of the hydrogels developed

### 2.4.1. Gel fraction and swelling experiments

Samples ( $\phi = 1.4$  mm, thickness = 1 mm) of the crosslinked hydrogels were incubated in double-distilled water at 37°C in order to determine the gel fraction of the crosslinked hydrogels. As a result, polymer chains that were not covalently linked into the network were able to leach out from the hydrogels by diffusion. The gel fraction can be calculated, expressed as the percentage of material which is chemically incorporated in the three-dimensional network (equation 1).

$$gel\ fraction\ (\%) = \frac{W_d}{W_{d0}} \cdot 100 \quad (1)$$

with  $W_d$  = dry weight after swelling  
 $W_{d0}$  = dry weight before swelling

All the measurements were performed in duplicate. The results are presented as mean values with corresponding standard deviations (SD).

For the swelling experiments, the hydrogel films were submerged in double-distilled water at 37°C, and the changes in mass were recorded as a function of time. At distinct time points, the

samples were removed from the medium, dipped on a piece of paper in order to remove adhered solution to the surface, and weighed. Afterwards, the samples were again incubated in the swelling medium.

The swelling percentage can be defined as:

$$Swelling (\%) = \frac{W_{ht} - W_{do}}{W_{do}} \cdot 100 \quad (2)$$

with  $W_{do}$  = weight of dry gel at initial time 0

$W_{ht}$  = weight of hydrated gel at time t

All these experiments were performed in duplicate. The results are reported as mean values with corresponding SD.

#### 2.4.2. Determination of crosslinking efficiency via HR-MAS $^1\text{H}$ -NMR spectroscopy

High Resolution Magic Angle Spinning  $^1\text{H}$  NMR spectroscopy (HR-MAS) was performed in order to evaluate the crosslinking efficiency (CE) of the developed hydrogel films. A Bruker Avance II 700 spectrometer (700.13 MHz) device was used applying a HR-MAS probe equipped with a  $^1\text{H}$ ,  $^{13}\text{C}$ ,  $^{119}\text{Sn}$  and gradient channel. The spinning rate was adjusted to 6 kHz.

On the day of the experiments, a small amount of the freeze-dried hydrogels was placed inside a 4 mm zirconium oxide MAS rotor (50  $\mu\text{l}$ ) and a few microliters of deuterium oxide ( $\text{D}_2\text{O}$ ) were added enabling the samples to swell. A teflon-coated cap was applied in order to close the rotor. Prior to analysis the HR-MAS samples were homogenized by manual stirring. Afterwards, the spectra were analyzed after baseline correction.

The CE is calculated using the following equation (Sandra Van Vlierberghe José C. Martins, and Peter Dubrue, 2010):

$$CE (\%) = \left[ \frac{\left( \frac{I_{5.75 \text{ or } 5.1 \text{ ppm}}^k}{I_{1.1 \text{ ppm}}^k} \right) - \left( \frac{I_{5.75 \text{ or } 5.1 \text{ ppm}}^c}{I_{1.1 \text{ ppm}}^c} \right)}{\left( \frac{I_{5.75 \text{ or } 5.1 \text{ ppm}}^k}{I_{1.1 \text{ ppm}}^k} \right)} \right] \times 100 \quad (3)$$

This equation (3) is based on the comparison of the intensity of the signals characterizing the protons of the introduced double bonds, before and after crosslinking. Normalization is applied by using the inert signal at 1.1 ppm, because different samples need to be compared.

#### 2.4.3. Rheology



The mechanical properties of the hydrogels were investigated via oscillation rheology with a rheometer type Physica MCR-301 (Anton Paar, Sint-Martens-Latem, Belgium) running with Physica Rheoplus software. All measurements were performed using a plate-plate geometry. More specifically, a hydrogel sample was placed between two parallel plates (diameter upper plate = 25 mm), after which the upper plate was adjusted to ensure close contact of each sample with both plates. Tests were performed using oscillatory sine functions and upon applying a frequency of 1 Hz and a gap setting of 0.95 mm. In addition, a 0.05% strain was selected to perform the oscillatory measurements as the linear visco-elastic range ranges from 0 to about 0.3% strain (data not shown). In the present work, the different hydrogels were measured under these settings while monitoring the storage ( $G'$ ) and the loss moduli ( $G''$ ).

#### 2.4.4. Atomic Force Microscopy and IR-mapping

Atomic force microscopy (AFM) experiments were performed with a Nanoscope IIIa Multimode (Digital Instruments, Santa Barbara, California, USA) applying 'tapping mode' in air. Measurements were performed on spincoated gelatin/starch solutions (10 w/v % gelatin and 5 w/v% starch solution) since AFM measurements require flat surfaces. In addition, spincoated gelatin and starch solutions were also measured separately as references. The nanoscope software version 4.43r8 was used to process all data obtained with AFM. On the other hand, IR-mapping was performed on dried hydrogel films using a Perkin Elmer Spectrum 100 FT-IR spectrometer with a Spotlight 400 FT-IR imaging system. Therefore, the hydrogel surfaces were scanned using IR mapping to evaluate the absorbance potentially occurring at the characteristic wavenumbers for gelatin and starch in order to determine the presence of both building blocks in the hydrogel samples."

Formatted: Font: (Default) Times New Roman, 12 pt

Formatted: Font: (Default) Times New Roman, 12 pt

### 2.5. Characterization of bioactive coating

In the present work, AFM and radiolabeling experiments were utilized in order to determine the interaction between gelatin and aggrecan.

#### 2.5.1. AFM under liquid conditions

AFM experiments were conducted on an Agilent 5500 AFM/SPM microscope in a liquid environment at 20 °C.

##### 2.5.1.1. Topographic AFM imaging

Prior to AFM imaging, aggrecan from bovine plasma was dissolved in phosphate buffered saline (PBS) to acquire a stock solution of 1 mg/ml. The aggrecan solution was diluted to the desired

concentration and added onto the gelatin hydrogel film for 30 minutes at room temperature followed by three PBS washing steps prior to imaging. The washing steps were essential to remove loosely bound aggrecan.

Images were obtained in tapping mode using silicon tips (Nanosensors, series PPP-NCSTR-50) with a resonance frequency within a range from 76 to 263 kHz and a force constant of 12 – 29 N/m. Typical scan rates were in the range of 0.5 – 1 kHz at a resolution of 512 points/line. All measurements were performed in PBS.

#### **2.5.1.2. Force spectroscopy**

Force spectroscopy measurements were performed using a backside aluminium coated silicon cantilever (Cont GB-G, Budget Sensor) with a nominal spring constant of 0.02 N/m and a resonant frequency of 13 kHz. Accurate measurement of spring constants was obtained using the equipartition theorem (Thermal K)(Hutter & Bechhoefer, 1993). Forces of interaction between the aggrecan and the hydrogel were measured by functionalizing the AFM tip with aggrecan through a physisorption process by incubation of the tip for 30 minutes. Prior to monitoring the aggrecan interactions with the gel, force distance curves were acquired on bare mica in order to confirm that the tip was successfully functionalized. Force spectroscopy experiments were performed on the gelatin samples at four locations defined by the user. Approximately 1000 – 1500 force-distance curves were obtained per location.

For the analysis of the data obtained, Scanning Probe Image Processor (SPIP) version 6.2.8 (Image Metrology, Lyngby, Denmark) was used. Interaction forces between the aggrecan and the gel were derived from the registered force distance curves. Histograms of the height features as well as the rupture forces were created with Sigmaplot (Systat Software, San Jose, CA). For the rupture force distributions of aggrecan, the selected curves were fitted to a Gaussian function in order to extract the average rupture force.

#### **2.5.2. Radiolabeling experiments**

Radioiodination was performed by a slightly modified method described by Pierce Biotechnology Inc. (Rockford, IL, USA; [www.piercenet.com](http://www.piercenet.com)). In brief: Iodogen was dissolved in chloroform to a concentration of 2 mg/mL and 100 µL was added to a 5 mL conical vial. The solvent was then evaporated under a gentle N<sub>2</sub> flow at room temperature and the Iodogen-coated vials were stored in a dessicator at 5 °C prior to use. A stock solution of aggrecan (0.5 mg/mL, 1.5 mL) was added to a Iodogen coated reaction vessel, immediately followed by the addition of 20 µL radioiodide solution (<sup>125</sup>I). This mixture was incubated for 20 minutes at room temperature under slight shaking. Free iodine was removed by G-25 Sephadex gel filtration (GE Healthcare, Belgium), equilibrated with 0.01 M phosphate buffer of pH 7. The overall radiochemical purity (RCP) was then determined using iTLC-SG chromatographic strips (Gel-man Sciences) and a citrate-buffer

(0.068 M citrate, pH 7.4) as eluent. From this  $^{125}\text{I}$ -aggrecan solution dilutions were prepared to adjust the concentration of aggrecan to 0.5, 0.3, 0.2, 0.1 and 0.05 mg/mL. The procedure for coating the hydrogel films is similar to the aforementioned in section 1.5.1.1.

### 3. Results and discussion

#### 3.1 In-depth physico-chemical characterization of the hydrogels

Gelatin and starch were modified with UV-crosslinkable side-groups enabling their subsequent processing into hydrogel films. Gelatin was successfully modified with varying amount of methacrylic anhydride.(Peters et al., 2009; Salamon et al., 2014) In this way, the influence of the DS on the mechanical properties could be evaluated. The modification was confirmed and quantified via  $^1\text{H}$ -NMR spectroscopy for the different gelatin derivatives (see figure S1). The methacrylamide-modified gelatins (gel-MA) in the present work possess a DS of 31, 72 and 95% with respect to the primary amines available along the gelatin backbone. In addition to the functionalized gelatin, starch was successfully modified using 4-pentenoic anhydride yielding starch-pentenoate (SP) with a DS of 32%.(Van Nieuwenhove et al., 2015) This DS was also quantified by means of  $^1\text{H}$ -NMR spectroscopy and is expressed as the amount of modified repeating saccharide units (see figure S1).

Subsequently, hydrogel films of both gel-MA and gel-MA in combination with SP were prepared via film casting followed by chemical crosslinking. This enabled the characterization of the developed materials via several techniques. Pure starch hydrogels were not developed as these hydrogels were not robust enough to enable manipulation.

##### 3.1.1. Gel fraction and swelling experiments

First, the gel fractions and the equilibrium swelling degree of the developed materials were determined. The results are listed in table 1 and to facilitate further discussion each hydrogel sample is designated with a unique code. On the one hand, gel-MA x% indicates hydrogels purely based on gelatin which are characterized by their DS represented by x%. On the other hand, the abbreviation SP1 reflects the presence of a SP content of 10% and SP2 assigns the IPNs defined by 20% SP content. The gel fraction results indicate an efficient crosslinking during which most of the crosslinkable moieties were consumed resulting in gel fractions of 85% and higher. In general, thus, well-established networks were formed as almost no leaching occurred of unbound molecules. As anticipated, it can be observed in table 1 that the gel fraction will increase with an increasing DS for gelatin hydrogels. This because a higher DS will result in a more crosslinked hydrogel network going from gel-MA 31% to 95%.

A small decrease in the gel fraction can be observed for the hydrogel samples with a starch content of 20% compared to 10% and the hydrogels without starch. However, conversely, an

increase in total amount of crosslinkable moieties is noticeable with an increasing amount of starch present in the polymer network (see last column table 1). It can be hypothesized that upon the introduction of a critical amount of starch (i.e. 20%), the phase separation between starch and gelatin will be more pronounced causing the starch to be more clustered together in domains. The occurrence of phase separation will still be tackled in depth in section 2.1.4.

Therefore, it is hypothesized that upon introducing this critical amount of starch the gel fraction again decreases because the starch domains leach out during incubation (cfr. these domains can be considered as starch-only hydrogels, which do not enable manipulation as already indicated above). This effect is not demonstrated in the hydrogel samples with a 10% starch content, since the starch hydrogel building blocks will be more randomly distributed in a gelatin phase.

The swelling experiments show that all hydrogel types are able to absorb large quantities of water. Indeed, equilibrium swelling degrees ranging from 660% up to 4100% were observed for the hydrogel samples developed. These results are in good agreement with the results obtained by Graulus et al. (2015) for gelatin hydrogels and hydrogels consisting of gelatin and alginate.(Graulus et al., 2015)

349 **Table 1** Gel fractions (%) for the various hydrogel samples and the number of crosslinkable moieties present in the precursor solutions (methacrylamide for gel-MA  
350 versus pentenoate for the starch phase). All measurements were performed in duplicate and the results are presented as mean values with corresponding standard  
351 deviations (SD) (n=2).

Code	Composition (v%)		Gel fraction (%) ± SD	mol MA moieties / ml precursor solution	mol pentenoate moieties / ml precursor solution	mol total amount of crosslinkable moieties/ ml precursor solution
	gel-MA	SP				
gel-MA 31%	100	-	85 ± 5	1.19E-05	-	1.19E-05
gel-MA 72%	100	-	94 ± 1	2.77E-05	-	2.77E-05
gel-MA 72% - SP1	90	10	100 ± 1	2.49E-05	9.87E-06	3.48E-05
gel-MA 72% - SP2	80	20	86 ± 4	2.22E-05	1.97E-05	4.19E-05
gel-MA 95%	100	-	98 ± 1	3.66E-05	-	3.66E-05
gel-MA 95% - SP1	90	10	100 ± 9	3.29E-05	9.87E-06	4.28E-05
gel-MA 95% - SP2	80	20	93 ± 7	2.93E-05	1.97E-05	4.90E-05

352

353

354

355

356

357

358

### 3.1.2. Evaluation of crosslinking efficiency

The crosslink efficiency (CE) of the UV-cured hydrogels was evaluated by means of HR-MAS  $^1\text{H}$ -NMR spectroscopy. This technique evaluates the consumption of double bonds upon crosslinking and is thus a measure for the efficiency of crosslinking. (Sandra Van Vlierberghe José C. Martins, and Peter Dubruel, 2010) Conventional  $^1\text{H}$ -NMR spectroscopy does not enable the characterization of crosslinked polymer networks due to the considerable line broadening which results from the presence of dipolar couplings and magnetic susceptibility effects. (Ramadhar, Amador, Ditty, & Power, 2008; Shapiro, Chin, Marti, & Jarosinski, 1997) HR-MAS spectroscopy circumvents this line broadening by rapidly rotating the sample at a magic angle of  $54.7^\circ$  with respect to the static magnetic field, following swelling of the material. (Ramadhar et al., 2008) This swelling induces sufficient, solution-like, rotational mobility of the polymer. (Sandra Van Vlierberghe José C. Martins, and Peter Dubruel, 2010) Highly crosslinked hydrogel materials will thus exhibit a reduced chain mobility and will show broader peaks compared to less crosslinked materials. (Rueda, Suica, Komber, & Voit, 2003)

The CE could only be calculated for the gelatin phase based on equation (3). Unfortunately, the CE of the starch phase could not be calculated separately due to overlap of the characteristic peaks of the starch and gelatin phase both present in the IPNs. Therefore, equation (3) is only applicable for the gelatin phase present in the IPNs. It is important to emphasize that the CE reflects a ratio between the amount of double bounds consumed upon crosslinking to the amount initially present in the samples.

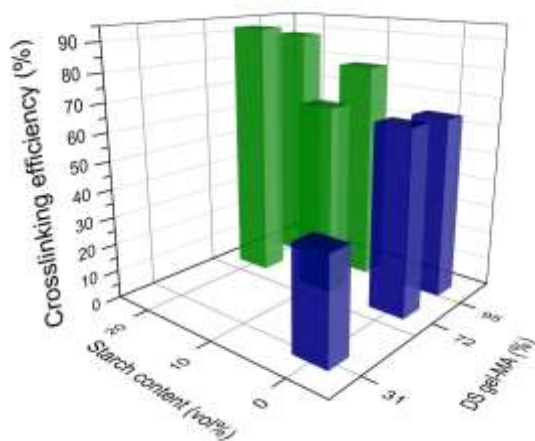


Figure 2 3D-plot representing the gelatin crosslinking efficiency (CE, z-axis) (%) of the various hydrogel films as a function of the starch content (x-axis) and the degree of substitution of methacrylamide-modified gelatin (gel-MA) hydrogels (axis).

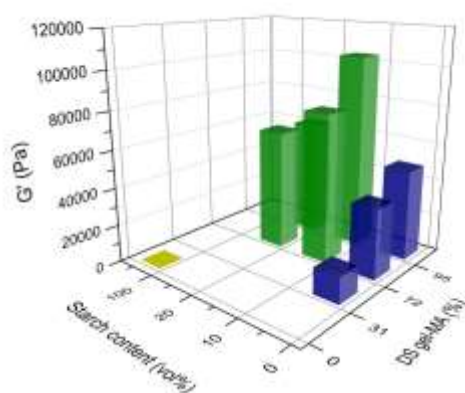
386 The CE values of the applied gelatin phase for the various hydrogel films are represented in  
 387 figure 2. In addition to these results, table 2 represents the calculated amount of network points  
 388 present in the gelatin phase taking into account the amount of photocrosslinkable MA side groups  
 389 present in the network and the CE.  
 390 The results for the pure gelatin hydrogels are in good correlation with previous reported results  
 391 for hydrogels crosslinked under similar conditions.(Salamon et al., 2014) However, the latter  
 392 paper did not comprise a comparison of different DS of gel-MA. Figure 2 indicates an increasing  
 393 CE with increasing DS for the hydrogels solely consisting of a gelatin phase (blue bars). This  
 394 increase is observed until a maximum in CE is reached at a DS of 72%, since the crosslinking  
 395 efficiencies for gel-MA 72% and 95% are in the same range. The trend of increasing CE with  
 396 increasing DS can be anticipated as more crosslinkable side groups will be incorporated along the  
 397 backbone for a higher DS (see table 2). Thus, more double bonds will be in closer proximity, and,  
 398 therefore more likely to react upon photo-crosslinking. Moreover, the CE remains similar  
 399 between the pure gelatin film compared to the IPNs with a 10% starch content (SP1 hydrogel  
 400 samples in table 2). An increase in CE is observed, however, upon addition of a 20% starch  
 401 phase. The latter phenomenon is anticipated to be the result of a more pronounced phase  
 402 separation occurring between starch and gelatin present in the IPNs which is more likely to occur  
 403 for the SP2 gelatin-starch IPNs as already highlighted in the previous section. This phase  
 404 separation ensures the gelatin chains to exist in closer proximity despite the presence of an  
 405 additional starch phase within the polymer network.  
 406  
 407

Table 2 Comparison of the amount of networks points in the gelatin phase with the amount of crosslinkable moieties in this gelatin phase for the various gelatin hydrogels samples developed as well as the interpenetrating networks based on gelatin and starch.

Code	mol MA moieties/ ml precursor solution	CE (%)	mol MA network points/ ml precursor solution
3.1.3. gel-MA 31%	1.19E-05	37	4.39E-06
gel-MA 72%	2.77E-05	65	1.82E-05
gel-MA 72% - SP1	2.49E-05	67	1.68E-05
gel-MA 72% - SP2	2.22E-05	92	2.04E-05
gel-MA 95%	3.66E-05	64	2.35E-05
gel-MA 95% - SP1	3.29E-05	79	2.59E-05
gel-MA 95% - SP2	2.93E-05	88	2.58E-05
m			
ination of mechanical properties			

418 Rheology was applied to examine the mechanical properties of the developed hydrogels. Polymer  
 419 materials typically exhibit visco-elastic behavior which implies that a recovery occurs at a certain  
 420 delay after deformation. As anticipated, an improvement in mechanical properties is observed for  
 421 more densely crosslinked hydrogels.(Hutson et al., 2011; Nichol et al., 2010; Van Den Bulcke et  
 422 al., 2000; Wang et al., 2014) This trend can be derived from figure 3 for the gel-MA and gel-MA  
 423 SP1 series along the y-axis: the storage modulus ( $G'$ ) increases with increasing DS of gel-MA.

424



425

426 Figure 3 3D plot representing the storage modulus  $G'$  of the various hydrogels (z-axis) as a function of the starch content (%)  
 427 (x-axis) and the degree of substitution of methacrylamide-modified gelatin (gel-MA) (y-axis).

428 Although HR-MAS  $^1\text{H}$  NMR spectroscopy indicated the highest CE for  
 429 gel-MA 72%, there is a lower absolute number of network points present compared to  
 430 gel-MA 95% (see last column table 2). Therefore, the hydrogel films consisting of gel-MA 95%  
 431 are characterized by a higher  $G'$ -value as these networks are more crosslinked. Moreover,  $G'$   
 432 shifts to higher values for the IPNs with a starch-content of 10%. The mechanical properties are  
 433 thus improved upon introducing an additional starch phase in the gelatin network. For the IPNs  
 434 with 10% starch content (SP1), the trend along the y-axis remains similar:  $G'$  increases with  
 435 increasing DS of gel-MA. A more crosslinked gelatin phase thus results in improved mechanical  
 436 properties. Conversely, the IPNs with 20% starch content (SP2) again exhibit lower  $G'$  values  
 437 than the IPNs with 10% starch (SP1). It can be anticipated that the addition of a critical amount  
 438 of starch will result in a more pronounced phase separation, as already indicated above. In  
 439 addition, the gel fraction results complement the data and trends as derived from rheology.

#### 440 3.1.4. Topographical characterization

441 The gelatin-starch IPNs were further investigated by AFM and IR mapping in order to study  
 442 relevant phase separation phenomena.(Dazzi et al., 2012; Ferrer, Sánchez, Ribelles, Colomer, &



Pradas, 2007) First of all, AFM is applied, a technique being part of the family of scanning probe microscopes which scan across a surface monitoring probe-sample interactions. The measurements were performed on spincoated gelatin/starch-solutions, since AFM experiments require flat surfaces. In addition, spincoated gelatin and starch-solutions were also measured separately as reference.

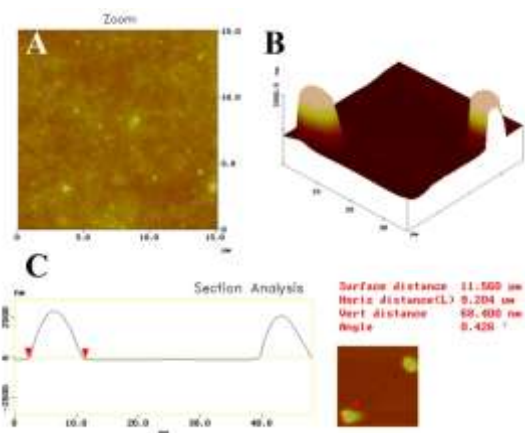


**Figure 4** A. Top view of methacrylamide-modified gelatin (gel-MA) B. 3D surface plot of 90% gel-MA + 10% starch-pentenoate C. Section analysis of starch granules present in a gelatin matrix.

The mixtures of gelatin and starch explicitly show smaller regions of phase-separated starch granules being present adjacent to the globular domains of gelatin. These granules are separate domains possessing a size of approximately 10  $\mu\text{m}$  (figure 4).

In addition to AFM, the incorporation of starch in the gelatin matrix was also evaluated by means of IR mapping of the characteristic wavenumbers of either gelatin (eg. 1633  $\text{cm}^{-1}$ ) or starch (eg. 1017 and 1079  $\text{cm}^{-1}$ ). The results of the air-dried gel-MA 72%-SP1 hydrogel are depicted in figure 5, together with the ATR-IR spectra of the starting materials. The results obtained from IR mapping clearly confirm the phase separation occurring between gelatin and starch. A separate starch domain was observed in the gelatin matrix exhibiting absorbance at the characteristic wavenumbers corresponding with C-O bond stretching. Moreover, the size of this starch domain is around 10  $\mu\text{m}$ , which is in correlation with the AFM data (figure 4). Phase separation between mixtures of gelatin and starch was already reported earlier.(Firoozmand et al., 2009; Firoozmand, Murray, & Dickinson, 2012; Khomutov, Lashek, Ptitchkina, & Morris, 1995; Whitehouse, Ashby, Abeysekera, & Robards, 1996) This phenomenon is mainly depending on the thermal conditions, the carbohydrate molecular structure and the properties of the aqueous solution including temperature, pH and ionic strength.(Firoozmand et al., 2012) Firoozmand et al. (2009) also observed phase separation between gelatin and starch in high-sugar gelled systems

consisting of a constant gelatin content (7 wt%) and variable oxidized starch content (from 0 up to 6 wt%).(Firoozmand et al., 2009) For this specific type of system, a microstructure could be observed exhibiting both gelatin- and starch-rich regions with these regions ranging in size from a few micrometers up to twenty micrometers observed via optical microscopy. However, it is important to emphasize that the phase separation and the size of the domains was highly dependent on the specific thermal treatment of the samples.

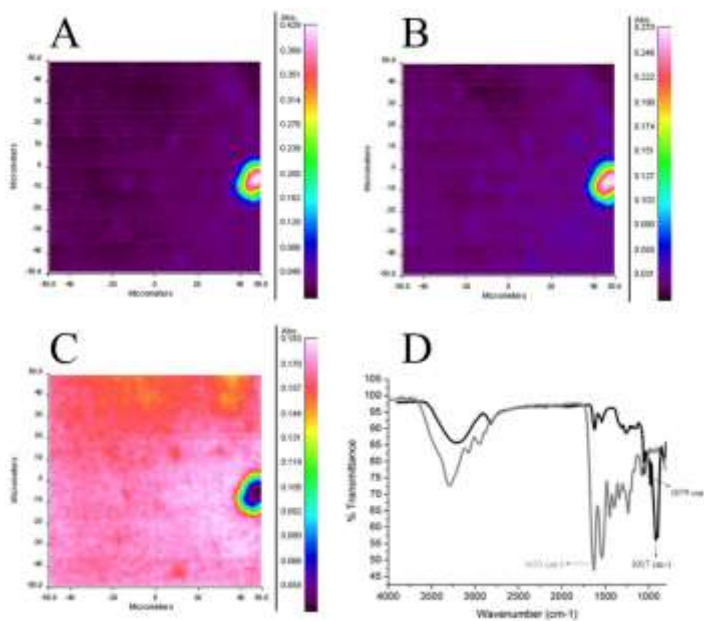


Figure 5 IR spectroscopy data of a dry gel-MA 72%-SP1 starch hydrogel film, including an IR map depicting the absorbance at A. 1017 cm<sup>-1</sup>, B. 1079 cm<sup>-1</sup>, C. 1633 cm<sup>-1</sup> and D. the ATR-IR spectra of gel-MA (light grey) and starch-pentenoate (dark grey).

### 3.2. Bioactive coating of gelatin hydrogels: aggrecan under investigation

The application of cell-interactive ECM-based coatings is crucial when it comes to tissue engineering, as these coatings can positively influence the cell growth(Altankov et al., 2000; Franck et al., 2013; Heller et al., 2015; Shin, Jo, & Mikos, 2003). In the present paper, aggrecan was selected as a component of the ECM to be applied on the gelatin hydrogels. To the best of our knowledge, no data is yet reported on the application of an aggrecan coating onto gelatin. Aggrecan is a major structural proteoglycan of the cartilage extracellular matrix with a molecular mass higher than 2500 kDa.(Kiani, Chen, Wu, Yee, & Yang, 2002) This molecule consists of numerous chondroitin and dermatan sulphate chains

491 attached to a core protein. In the present work, AFM and radiolabeling studies were performed in  
492 order to determine the interaction between gelatin and aggrecan.

493 First, AFM was selected to examine the interaction between aggrecan and gelatin, as it allows  
494 real-time imaging under liquid conditions, while providing a means to interrogate forces of  
495 interaction at picoNewton resolution. The coated gelatin hydrogels were visualized by means of  
496 tapping mode AFM before and after coating of the hydrogel surface with the proteoglycan (see  
497 figure 6). At a concentration of 50  $\mu\text{g/ml}$  of aggrecan, no distinct features appear in the  
498 topographic image of the coated hydrogel. Moreover, the height features detected are within the  
499 same range as a non-coated gelatin hydrogel sample (see figures 6A and 6B). Thus, for this  
500 concentration, no aggrecan can be detected on top of the gelatin hydrogels. The results from  
501 figure 6C clearly show that features between 1.5 and 3 nm and even up to 6 nm are present on the  
502 gelatin surface after aggrecan coating at a minimal concentration of 200  $\mu\text{g/ml}$ . For a  
503 concentration of 500  $\mu\text{g/ml}$ , a high number of features sized between 1.5 and 2.5 nm can be  
504 detected which indicates the presence of more aggrecan on the surface of the gelatin hydrogel.

505

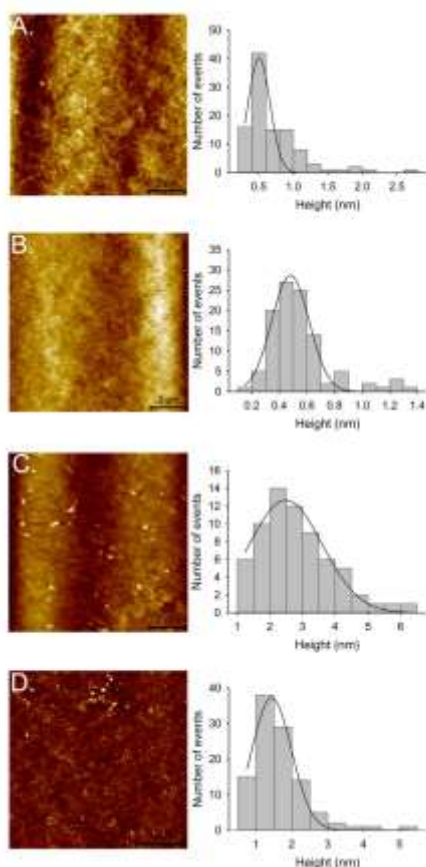


**Figure 6** Topographic atomic force microscopy images of spincoated, crosslinked methacrylamide-modified gelatin sample **A.** without aggrecan-coating and at an aggrecan concentration of **B.** 50  $\mu\text{g/ml}$ , **C.** 200  $\mu\text{g/ml}$ , and **D.** 500  $\mu\text{g/ml}$ . Images were obtained in liquid environment (PBS) at 20°C applying tapping mode.

Following topographic imaging of the surface, force spectroscopy experiments were performed to further characterize the gelatin-aggrecan affinity. For this reason, the operation mode was switched to contact mode and the AFM tip was functionalized with aggrecan. This procedure of tip functionalization via physical interactions allows dangling aggrecan molecules to be "pulled off" the surface that they are in contact with.(Florin et al., 1995) Figure 7 represents the force-distance curves obtained for the gel-MA samples and thus reflecting the adhesion force between aggrecan and gelatin. These forces of interaction between aggrecan and the hydrogel slightly increase from 0.97 to 1.25 nN with increasing DS of gel-MA. The forces detected are in the same range compared to the forces detected between proteins and biomaterial surfaces including

collagen and hyaluronic acid.(Donlon, Nordin, & Frankel, 2012; Herman-Bausier & Dufrene, 2016)

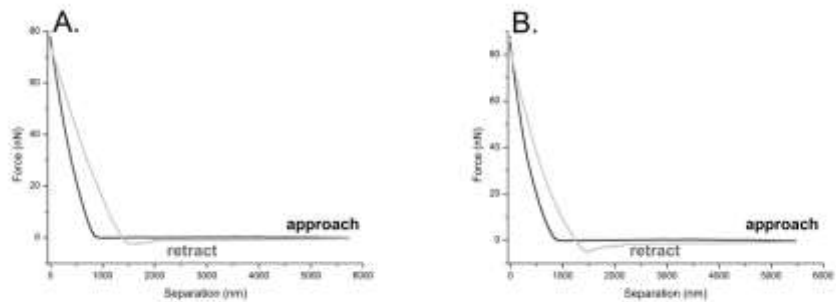


**Figure 7 Force spectroscopy experiments of functionalized aggrecan-AFM tip absorbed on spincoated methacrylamide-modified gelatin samples with a degree of substitution of A. 71 % , and B. 94 %**

In a second part of the affinity study, radiolabeling experiments were performed enabling the determination of the absolute mass of bound aggrecan. For these experiments, aggrecan was radiolabeled with  $^{125}\text{I}$ , and subsequently, a series of different concentrations of radiolabeled aggrecan was coated on top of the gelatin hydrogels. The experiments were performed in triplicate and the mean values and corresponding standard deviations are depicted in figure 8. The results clearly indicate a dose-responsive signal which is nearly linear within the studied concentration range from 50 to 500  $\mu\text{g/ml}$  aggrecan. It can be concluded that the radiolabeling experiments enable characterization of the aggrecan/gelatin affinity at lower concentrations (i.e. 50  $\mu\text{g/ml}$ ) than liquid AFM which could only visualize concentrations starting from 200  $\mu\text{g/ml}$  aggrecan.

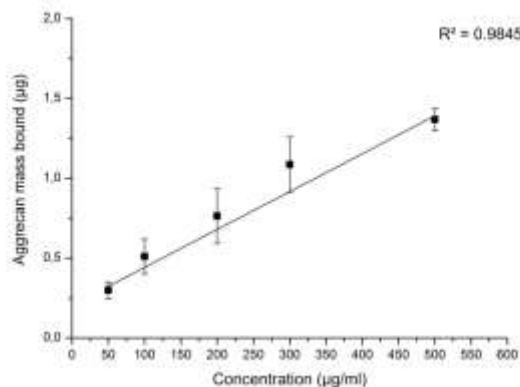


Figure 8 Adsorbed aggrecan amount (µg) as a function of the aggrecan concentration (µg/ml) applied on methacrylamide-modified gelatin measured by radiolabeling experiments.

#### 4. Conclusions

With the aim to investigate how the physico-chemical properties of biopolymer-based hydrogel films can be fine-tuned, hydrogel films were developed with varying chemical composition and degree of substitution of the functionalized gelatin. It can be concluded that the mechanical properties of the hydrogels can be fine-tuned depending on the degree of substitution of the methacrylamide-modified gelatin as well as the chemical composition (i.e. ratio gelatin/starch). The latter is reflected by the storage modulus of the developed materials which ranges from 14 to 63 kPa. Furthermore, phase separation was observed for the IPNs as separated starch domains were present in the gelatin matrix. In addition, the present work also aimed at studying the affinity of aggrecan for gelatin. This affinity was successfully demonstrated via liquid atomic force microscopy and radiolabelling experiments. Thus, it can be concluded that gelatin-based hydrogels can be coated with aggrecan via physisorption. [In a forthcoming paper, an \*in vitro\* cell assay will be performed using human mesenchymal stem cells in order to evaluate the adipogenic as well as osteogenic differentiation potential of the hydrogels developed herein](#)

~~In the subsequent 'part B' of this paper, all hydrogels developed will be evaluated for their potential to support adipose as well as osteogenic tissue regeneration in an *in vitro* approach based on human mesenchymal stem cells. In addition, the effectivity of a bioactive coating on top of the gelatin hydrogels films on these differentiation pathways will be assessed.~~

#### Acknowledgment

I. Van Nieuwenhove would like to thank Ghent University for the financial support with a doctoral fellowship 'BOF-mandaat' and the Research Foundation-Flanders (FWO, Belgium) for a travel grant (K213414N). S. Van Vlierberghe would like to acknowledge the FWO for

Formatted: Font: (Default) Times New Roman, 12 pt

595 financial support under the form of a research grant ('Development of the ideal tissue engineering  
596 scaffold by merging state-of-the-art processing techniques', FWO Krediet aan Navorsers) as well  
597 as Ghent University for the granted associate professorship. P. Dubruel would like to  
598 acknowledge the Alexander von Humboldt Foundation for the financial support under the form  
599 of a granted Research Fellowship. The 700 MHz used in this work was funded through the  
600 FFEU-ZWAP initiative of the Flemish Government and the Hercules foundation (grant number  
601 AUGÉ-09-006). All authors acknowledge the funding obtained for the EuroTransBio (ETB)  
602 Project ETB-2012-33 "Autologous Stem Cell-Enriched Scaffolds for Soft Tissue  
603 Regeneration—ASCaffolds".  
604

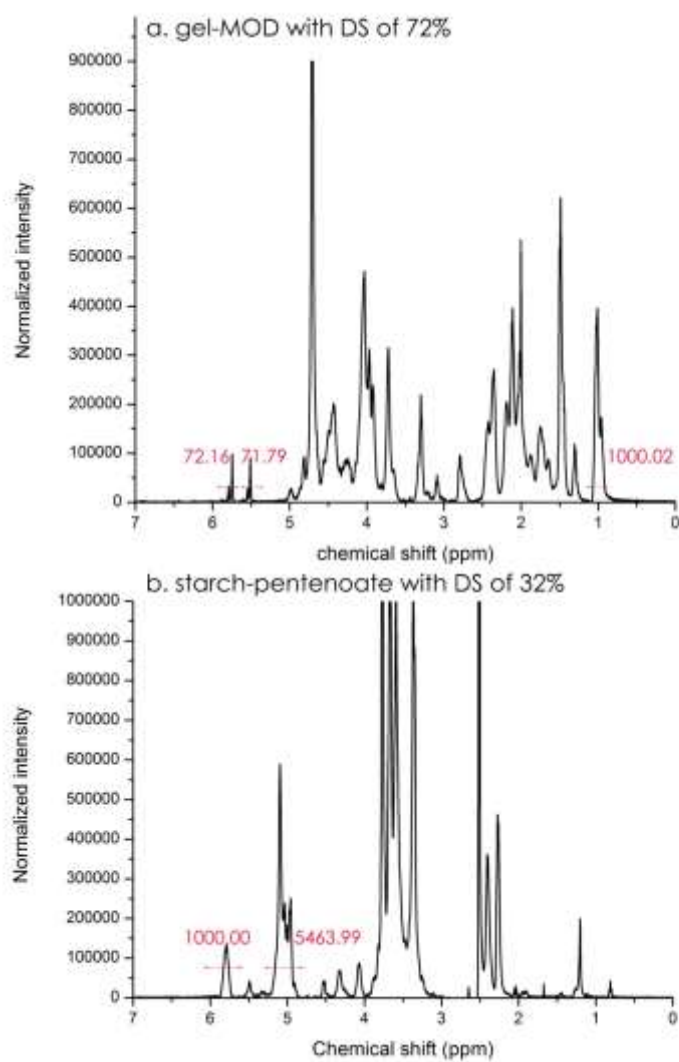


Figure S 1  $^1\text{H}$  NMR spectrum of a. gel-MA in  $\text{D}_2\text{O}$  at  $40^\circ\text{C}$ , b. starch-pentenoate in  $\text{DMSO}-d_6$  at  $60^\circ\text{C}$ .



609 Abbas, S., Judit, Z., & Donald, P. (2007). Elastic moduli of normal and pathological human breast tissues:  
610 an inversion-technique-based investigation of 169 samples. *Physics in Medicine and Biology*, 52(6),  
611 1565. Retrieved from <http://stacks.iop.org/0031-9155/52/i=6/a=002>

612 Altankov, G., Thom, V., Groth, T., Jankova, K., Jonsson, G., & Ulbricht, M. (2000). Modulating the  
613 biocompatibility of polymer surfaces with poly(ethylene glycol): Effect of fibronectin. *Journal of*  
614 *Biomedical Materials Research*, 52(1), 219–230. [http://doi.org/10.1002/1097-](http://doi.org/10.1002/1097-4636(200010)52:1<219::aid-jbm28>3.0.co;2-f)  
615 4636(200010)52:1<219::aid-jbm28>3.0.co;2-f

616 Awad, H. A., Quinn Wickham, M., Leddy, H. A., Gimble, J. M., & Guilak, F. (2004). Chondrogenic  
617 differentiation of adipose-derived adult stem cells in agarose, alginate, and gelatin scaffolds.  
618 *Biomaterials*, 25(16), 3211–3222. <http://doi.org/http://dx.doi.org/10.1016/j.biomaterials.2003.10.045>

619 Azevedo, H. S., Gama, F. M., & Reis, R. L. (2003). In Vitro Assessment of the Enzymatic Degradation of  
620 Several Starch Based Biomaterials. *Biomacromolecules*, 4(6), 1703–1712.  
621 <http://doi.org/10.1021/bm0300397>

622 Barry, F. P., & Murphy, J. M. (2004). Mesenchymal stem cells: clinical applications and biological  
623 characterization. *The International Journal of Biochemistry & Cell Biology*, 36(4), 568–584.  
624 <http://doi.org/http://dx.doi.org/10.1016/j.biocel.2003.11.001>

625 Burey, P., Bhandari, B. R., Rutgers, R. P. G., Halley, P. J., & Torley, P. J. (2009). Confectionery Gels: A  
626 Review on Formulation, Rheological and Structural Aspects. *International Journal of Food*  
627 *Properties*, 12(1), 176–210. <http://doi.org/10.1080/10942910802223404>

628 Chen, Z. G., Wang, P. W., Wei, B., Mo, X. M., & Cui, F. Z. (2010). Electrospun collagen–chitosan  
629 nanofiber: A biomimetic extracellular matrix for endothelial cell and smooth muscle cell. *Acta*  
630 *Biomaterialia*, 6(2), 372–382. <http://doi.org/http://dx.doi.org/10.1016/j.actbio.2009.07.024>

631 Cui, L., Jia, J., Guo, Y., Liu, Y., & Zhu, P. (2014). Preparation and characterization of IPN hydrogels  
632 composed of chitosan and gelatin cross-linked by genipin. *Carbohydrate Polymers*, 99, 31–38.  
633 <http://doi.org/http://dx.doi.org/10.1016/j.carbpol.2013.08.048>

634 Dazzi, A., Prater, C. B., Hu, Q., Chase, D. B., Rabolt, J. F., & Marcott, C. (2012). AFM&#8208;IR:  
635 Combining Atomic Force Microscopy and Infrared Spectroscopy for Nanoscale Chemical  
636 Characterization. *Applied Spectroscopy*, 66(12), 1365–1384. <http://doi.org/10.1366/12-06804>

637 Di Lullo, G. A., Sweeney, S. M., Korkko, J., Ala-Kokko, L., & San Antonio, J. D. (2002). Mapping the  
638 ligand-binding sites and disease-associated mutations on the most abundant protein in the human,  
639 type I collagen. *The Journal of Biological Chemistry*, 277(6), 4223–4231.  
640 <http://doi.org/10.1074/jbc.m110709200>

641 Donlon, L., Nordin, D., & Frankel, D. (2012). Complete unfolding of fibronectin reveals surface  
642 interactions. *Soft Matter*, 8(38), 9933–9940. <http://doi.org/10.1039/C2SM26315G>

643 Dragan, E. S. (2014). Design and applications of interpenetrating polymer network hydrogels. A review.  
644 *Chemical Engineering Journal*, 243, 572–590.  
645 <http://doi.org/http://dx.doi.org/10.1016/j.cej.2014.01.065>

646 Drury, J. L., & Mooney, D. J. (2003). Hydrogels for tissue engineering: scaffold design variables and  
647 applications. *Biomaterials*, 24(24), 4337–4351. [http://doi.org/http://dx.doi.org/10.1016/S0142-](http://doi.org/http://dx.doi.org/10.1016/S0142-9612(03)00340-5)  
648 9612(03)00340-5

649 Dubrue, P., Unger, R., Van Vlierberghe, S., Cnudde, V., Jacobs, P. J. S., Schacht, E., & Kirkpatrick, C. J.

650 (2007). Porous Gelatin Hydrogels: 2. In Vitro Cell Interaction Study. *Biomacromolecules*, 8(2),  
 651 338–344. <http://doi.org/10.1021/bm0606869>

652 Ferrer, G. G., Sánchez, M. S., Ribelles, J. L. G., Colomer, F. J. R., & Pradas, M. M. (2007). Nanodomains  
 653 in a hydrophilic–hydrophobic IPN based on poly(2-hydroxyethyl acrylate) and poly(ethyl acrylate).  
 654 *European Polymer Journal*, 43(8), 3136–3145.  
 655 <http://doi.org/http://dx.doi.org/10.1016/j.eurpolymj.2007.05.019>

656 Firoozmand, H., Murray, B. S., & Dickinson, E. (2009). Microstructure and rheology of phase-separated  
 657 gels of gelatin + oxidized starch. *Food Hydrocolloids*, 23(4), 1081–1088.  
 658 <http://doi.org/http://dx.doi.org/10.1016/j.foodhyd.2008.07.013>

659 Firoozmand, H., Murray, B. S., & Dickinson, E. (2012). Microstructure and elastic modulus of mixed gels  
 660 of gelatin + oxidized starch: Effect of pH. *Food Hydrocolloids*, 26(1), 286–292.  
 661 <http://doi.org/http://dx.doi.org/10.1016/j.foodhyd.2011.06.007>

662 Florin, E. L., Rief, M., Lehmann, H., Ludwig, M., Dornmair, C., Moy, V. T., & Gaub, H. E. (1995).  
 663 Sensing specific molecular interactions with the atomic force microscope. *Biosensors and*  
 664 *Bioelectronics*, 10(9–10), 895–901. [http://doi.org/http://dx.doi.org/10.1016/0956-5663\(95\)99227-C](http://doi.org/http://dx.doi.org/10.1016/0956-5663(95)99227-C)

665 Franck, D., Gil, E. S., Adam, R. M., Kaplan, D. L., Chung, Y. G., Estrada, C. R., & Mauney, J. R. (2013).  
 666 Evaluation of Silk Biomaterials in Combination with Extracellular Matrix Coatings for Bladder  
 667 Tissue Engineering with Primary and Pluripotent Cells. *PLoS ONE*, 8(2), e56237.  
 668 <http://doi.org/10.1371/journal.pone.0056237>

669 Furth, M. E., Atala, A., & Van Dyke, M. E. (2007). Smart biomaterials design for tissue engineering and  
 670 regenerative medicine. *Biomaterials*, 28(34), 5068–5073.  
 671 <http://doi.org/http://dx.doi.org/10.1016/j.biomaterials.2007.07.042>

672 Gautam, S., Dinda, A. K., & Mishra, N. C. (2013). Fabrication and characterization of PCL/gelatin  
 673 composite nanofibrous scaffold for tissue engineering applications by electrospinning method.  
 674 *Materials Science and Engineering: C*, 33(3), 1228–1235.  
 675 <http://doi.org/http://dx.doi.org/10.1016/j.msec.2012.12.015>

676 Gomillion, C. T., & Burg, K. J. L. (2006). Stem cells and adipose tissue engineering. *Biomaterials*,  
 677 27(36), 6052–6063. <http://doi.org/http://dx.doi.org/10.1016/j.biomaterials.2006.07.033>

678 Graulus, G.-J., Mignon, A., Van Vlierbergh, S., Declercq, H., Feher, K., Cornelissen, M., ... Dubrue, P.  
 679 (2015). Cross-linkable alginate-graft-gelatin copolymers for tissue engineering applications.  
 680 *EUROPEAN POLYMER JOURNAL*, 72, 494–506. <http://doi.org/10.1016/j.eurpolymj.2015.06.033>

681 Griffith, L. G., & Naughton, G. (2002). Tissue engineering--current challenges and expanding  
 682 opportunities. *Science*, 295(5557), 1009–1014. Retrieved from  
 683 <http://search.proquest.com/docview/213597341?accountid=11077>

684 Heller, M., Kämmerer, P. W., Al-Nawas, B., Luszpinski, M.-A., Förch, R., & Brieger, J. (2015). The  
 685 effect of extracellular matrix proteins on the cellular response of HUVECS and HOBS after covalent  
 686 immobilization onto titanium. *Journal of Biomedical Materials Research Part A*, 103(6), 2035–  
 687 2044. <http://doi.org/10.1002/jbm.a.35340>

688 Herman-Bausier, P., & Dufrene, Y. F. (2016). Atomic force microscopy reveals a dual collagen-binding  
 689 activity for the staphylococcal surface protein SdrF. *MOLECULAR MICROBIOLOGY*, 99(3), 611–  
 690 621. <http://doi.org/10.1111/mmi.13254>

691 Hutson, C. B., Nichol, J. W., Aubin, H., Bae, H., Yamanlar, S., Al-Haque, S., ... Khademhosseini, A.  
692 (2011). Synthesis and Characterization of Tunable Poly(Ethylene Glycol): Gelatin Methacrylate  
693 Composite Hydrogels. *Tissue Engineering Part A*, 17(13-14), 1713–1723.  
694 <http://doi.org/10.1089/ten.tea.2010.0666>

695 Hutter, J. L., & Bechhoefer, J. (1993). CALIBRATION OF ATOMIC-FORCE MICROSCOPE TIPS  
696 (VOL 64, PG 1868, 1993). *Review of Scientific Instruments*, 64(11), 3342.  
697 <http://doi.org/10.1063/1.1144449>

698 Jeffrey M. Gimble, Adam J. Katz, Bunnell, B. A., Gimble, J. M., Katz, A. J., & Bunnell, B. A. (2007).  
699 Adipose-derived stem cells for regenerative medicine. *Circulation Research*, 100(9), 1249–1260.  
700 <http://doi.org/10.1161/01.res.0000265074.83288.09>

701 Khomutov, L. I., Lashek, N. A., Ptitchkina, N. M., & Morris, E. R. (1995). Temperature-composition  
702 phase diagram and gel properties of the gelatin-starch-water system. *CARBOHYDRATE*  
703 *POLYMERS*, 28(4), 341–345. [http://doi.org/10.1016/0144-8617\(96\)00001-X](http://doi.org/10.1016/0144-8617(96)00001-X)

704 Kiani, C., Chen, L., Wu, Y. J., Yee, A. J., & Yang, B. B. (2002). Structure and function of aggrecan. *Cell*  
705 *Res*, 12(1), 19–32. Retrieved from <http://dx.doi.org/10.1038/sj.cr.7290106>

706 Kim, H.-W., Kim, H.-E., & Salih, V. (2005). Stimulation of osteoblast responses to biomimetic  
707 nanocomposites of gelatin–hydroxyapatite for tissue engineering scaffolds. *Biomaterials*, 26(25),  
708 5221–5230. <http://doi.org/http://dx.doi.org/10.1016/j.biomaterials.2005.01.047>

709 Kuo, C.-Y., Chen, C.-H., Hsiao, C.-Y., & Chen, J.-P. (2015). Incorporation of chitosan in biomimetic  
710 gelatin/chondroitin-6-sulfate/hyaluronan cryogel for cartilage tissue engineering. *Carbohydrate*  
711 *Polymers*, 117(0), 722–730. <http://doi.org/http://dx.doi.org/10.1016/j.carbpol.2014.10.056>

712 La Gatta, A., Schiraldi, C., Esposito, A., D'Agostino, A., & De Rosa, A. (2009). Novel poly(HEMA-co-  
713 METAC)/alginate semi-interpenetrating hydrogels for biomedical applications: Synthesis and  
714 characterization. *Journal of Biomedical Materials Research Part A*, 90A(1), 292–302.  
715 <http://doi.org/10.1002/jbm.a.32094>

716 Langer R, V. J. P. (1993). Tissue Engineering. *Science*, 260(5110), 920–926.

717 Langer, R. (1997). Tissue Engineering: A New Field and Its Challenges . *Pharmaceutical Research*,  
718 14(7)(7), 840–841.

719 Lemons, B. D. R. S. H. J. S. E. (Ed.). (2013). SECTION II.6 - Applications of Biomaterials in Functional  
720 Tissue Engineering. In *Biomaterials Science (Third Edition)* (pp. 1119–1122). Academic Press.  
721 <http://doi.org/http://dx.doi.org/10.1016/B978-0-08-087780-8.00108-X>

722 Li, M., Mondrinos, M. J., Gandhi, M. R., Ko, F. K., Weiss, A. S., & Leikes, P. I. (2005). Electrospun  
723 protein fibers as matrices for tissue engineering. *Biomaterials*, 26(30), 5999–6008.  
724 <http://doi.org/http://dx.doi.org/10.1016/j.biomaterials.2005.03.030>

725 Liu, C., Xia, Z., & Czernuszka, J. T. (2007). Design and Development of Three-Dimensional Scaffolds for  
726 Tissue Engineering. *Chemical Engineering Research and Design*, 85(7), 1051–1064.  
727 <http://doi.org/http://dx.doi.org/10.1205/cherd06196>

728 Liu, Y., & Chan-Park, M. B. (2009). Hydrogel based on interpenetrating polymer networks of dextran and  
729 gelatin for vascular tissue engineering. *Biomaterials*, 30(2), 196–207.  
730 <http://doi.org/http://dx.doi.org/10.1016/j.biomaterials.2008.09.041>

731 Lutolf, M. P., & Hubbell, J. A. (2005). Synthetic biomaterials as instructive extracellular  
 732 microenvironments for morphogenesis in tissue engineering. *Nature Biotechnology*, 23(1), 47–55.  
 733 <http://doi.org/http://dx.doi.org/10.1038/nbt1055>

734 MARRS, W. M. (1982). GELATIN CARBOHYDRATE INTERACTIONS AND THEIR EFFECT ON  
 735 THE STRUCTURE AND TEXTURE OF CONFECTIONERY GELS. *PROGRESS IN FOOD AND*  
 736 *NUTRITION SCIENCE*, 6(1-6), 259–268.

737 Mendes, S. C., Reis, R. ., Bovell, Y. P., Cunha, A. ., van Blitterswijk, C. A., & de Bruijn, J. D. (2001).  
 738 Biocompatibility testing of novel starch-based materials with potential application in orthopaedic  
 739 surgery: a preliminary study. *Biomaterials*, 22(14), 2057–2064. [http://doi.org/10.1016/S0142-](http://doi.org/10.1016/S0142-9612(00)00395-1)  
 740 [9612\(00\)00395-1](http://doi.org/10.1016/S0142-9612(00)00395-1)

741 Nichol, J. W., Koshy, S. T., Bae, H., Hwang, C. M., Yamanlar, S., & Khademhosseini, A. (2010). Cell-  
 742 laden microengineered gelatin methacrylate hydrogels. *Biomaterials*, 31(21), 5536–5544.  
 743 <http://doi.org/http://dx.doi.org/10.1016/j.biomaterials.2010.03.064>

744 Peng, C.-K., Yu, S.-H., Mi, F.-L., & Shyu, S.-S. (2006). Polysaccharide-based artificial extracellular  
 745 matrix: Preparation and characterization of three-dimensional, macroporous chitosan and chondroitin  
 746 sulfate composite scaffolds. *Journal of Applied Polymer Science*, 99(5), 2091–2100.  
 747 <http://doi.org/10.1002/app.22730>

748 Pescosolido, L., Piro, T., Vermonden, T., Coviello, T., Alhaique, F., Hennink, W. E., & Matricardi, P.  
 749 (2011). Biodegradable IPNs based on oxidized alginate and dextran-HEMA for controlled release of  
 750 proteins. *Carbohydrate Polymers*, 86(1), 208–213.  
 751 <http://doi.org/http://dx.doi.org/10.1016/j.carbpol.2011.04.033>

752 Peters, K., Salamon, A., Van Vlierberghe, S., Rychly, J., Kreutzer, M., Neumann, H.-G., ... Dubrue, P.  
 753 (2009). A New Approach for Adipose Tissue Regeneration Based on Human Mesenchymal Stem  
 754 Cells in Contact to Hydrogels—an In Vitro Study. *Advanced Engineering Materials*, 11(10), B155–  
 755 B161. <http://doi.org/10.1002/adem.200800379>

756 Picard, J., Doumèche, B., Panouillé, M., & Larreta-Garde, V. (2010). Gelatin-Polysaccharide Mixed  
 757 Biogels: Enzyme-Catalyzed Dynamics and IPNs. *Macromolecular Symposia*, 291-292(1), 337–344.  
 758 <http://doi.org/10.1002/masy.201050540>

759 Puppi, D., Chiellini, F., Piras, A. M., & Chiellini, E. (2010). Polymeric materials for bone and cartilage  
 760 repair. *Progress in Polymer Science*, 35(4), 403–440.  
 761 <http://doi.org/http://dx.doi.org/10.1016/j.progpolymsci.2010.01.006>

762 Raafat, A. I., Eldin, A. A. S., Salama, A. A., & Ali, N. S. (2013). Characterization and bioactivity  
 763 evaluation of (starch/N-vinylpyrrolidone)hydroxyapatite nanocomposite hydrogels for bone tissue  
 764 regeneration. *JOURNAL OF APPLIED POLYMER SCIENCE*, 128(3), 1697–1705.  
 765 <http://doi.org/10.1002/app.38113>

766 Ramadhar, T. R., Amador, F., Ditty, M. J. T., & Power, W. P. (2008). Inverse H-C ex situ HRMAS NMR  
 767 experiments for solid-phase peptide synthesis. *Magnetic Resonance in Chemistry*, 46(1), 30–35.  
 768 <http://doi.org/10.1002/mrc.2118>

769 Rueda, J., Suica, R., Komber, H., & Voit, B. (2003). Synthesis of New Polymethyloxazoline Hydrogels by  
 770 the “Macroinitiator” Method. *Macromolecular Chemistry and Physics*, 204(7), 954–960.  
 771 <http://doi.org/10.1002/macp.200390065>

772 Salamon, A., van Vlierberghe, S., van Nieuwenhove, I., Baudisch, F., Graulus, G.-J., Benecke, V., ...  
 773 Peters, K. (2014). Gelatin-Based Hydrogels Promote Chondrogenic Differentiation of Human  
 774 Adipose Tissue-Derived Mesenchymal Stem Cells In Vitro. *Materials*, 7(2), 1342–1359.  
 775 <http://doi.org/10.3390/ma7021342>

776 Sandra Van Vlierberghe José C. Martins, and Peter Dubruel, B. F. (2010). Hydrogel Network Formation  
 777 Revised: High-Resolution Magic Angle Spinning Nuclear Magnetic Resonance as a Powerful Tool  
 778 for Measuring Absolute Hydrogel Cross-Link Efficiencies. *Applied Spectroscopy*, 64(10), 1176–  
 779 1180.

780 Shapiro, M. J., Chin, J., Marti, R. E., & Jarosinski, M. A. (1997). Enhanced resolution in MAS NMR for  
 781 combinatorial chemistry. *Tetrahedron Letters*, 38(8), 1333–1336.  
 782 [http://doi.org/http://dx.doi.org/10.1016/S0040-4039\(97\)00092-0](http://doi.org/http://dx.doi.org/10.1016/S0040-4039(97)00092-0)

783 Shin, H., Jo, S., & Mikos, A. G. (2003). Biomimetic materials for tissue engineering. *Biomaterials*,  
 784 24(24), 4353–4364. [http://doi.org/http://dx.doi.org/10.1016/S0142-9612\(03\)00339-9](http://doi.org/http://dx.doi.org/10.1016/S0142-9612(03)00339-9)

785 Silver, F. H., Bradica, G., & Tria, A. (2002). Elastic energy storage in human articular cartilage:  
 786 estimation of the elastic modulus for type II collagen and changes associated with osteoarthritis.  
 787 *Matrix Biology*, 21(2), 129–137. [http://doi.org/http://dx.doi.org/10.1016/S0945-053X\(01\)00195-0](http://doi.org/http://dx.doi.org/10.1016/S0945-053X(01)00195-0)

788 Turgeon, S. L., & Beaulieu, M. (2001). Improvement and modification of whey protein gel texture using  
 789 polysaccharides. *Food Hydrocolloids*, 15(4–6), 583–591.  
 790 [http://doi.org/http://dx.doi.org/10.1016/S0268-005X\(01\)00064-9](http://doi.org/http://dx.doi.org/10.1016/S0268-005X(01)00064-9)

791 V, A. J., V, C. A., J, H., M, H., K, H., G, J. R., ... T, S. R. F. (2007). Definitions of terms relating to the  
 792 structure and processing of sols, gels, networks, and inorganic-organic hybrid materials (IUPAC  
 793 Recommendations 2007). *Pure and Applied Chemistry*. <http://doi.org/10.1351/pac200779101801>

794 Van Den Bulcke, A. I., Bogdanov, B., De Rooze, N., Schacht, E. H., Cornelissen, M., & Berghmans, H.  
 795 (2000). Structural and Rheological Properties of Methacrylamide Modified Gelatin Hydrogels.  
 796 *Biomacromolecules*, 1(1), 31–38. <http://doi.org/10.1021/bm990017d>

797 Van Nieuwenhove, I., Van Vlierberghe, S., Salamon, A., Peters, K., Thienpont, H., & Dubruel, P. (2015).  
 798 Photo-crosslinkable biopolymers targeting stem cell adhesion and proliferation: the case study of  
 799 gelatin and starch-based IPNs. *Journal of Materials Science: Materials in Medicine*, 26(2), 104.  
 800 <http://doi.org/10.1007/s10856-015-5424-4>

801 Wang, H., Zhou, L., Liao, J., Tan, Y., Ouyang, K., Ning, C., ... Tan, G. (2014). Cell-laden  
 802 photocrosslinked GelMA-DexMA copolymer hydrogels with tunable mechanical properties for  
 803 tissue engineering. *JOURNAL OF MATERIALS SCIENCE-MATERIALS IN MEDICINE*, 25(9),  
 804 2173–2183. <http://doi.org/10.1007/s10856-014-5261-x>

805 Whitehouse, A. S., Ashby, P., Abeysekera, R., & Robards, A. W. (1996). Phase behaviour of biopolymers  
 806 at high solid concentrations. In Phillips, GO and Williams, PA and Wedlock, DJ (Ed.), *GUMS AND*  
 807 *STABILISERS FOR THE FOOD INDUSTRY 8* (pp. 287–295). OXFORD UNIVERSITY PRESS  
 808 GREAT CLAREDON ST, OXFORD OX2 6DP, ENGLAND: IRL PRESS.

809